JOURNAL OF THERMOPHYSICS AND HEAT TRANSFER
Vol. 23, No. 3, July–September 2009

Simple Numerical Method for Multidimensional Inverse Identification of Heat Flux Distribution

Chunli Fan,* Fengrui Sun,† and Li Yang†
Naval University of Engineering, 430033 Wuhan, People's Republic of China

DOI: 10.2514/1.38446

In this paper, the inverse heat conduction problem is solved for the identification of the distribution of the heat flux applied to a flat plate based on the surface temperature measurement at the opposite boundary. The modified one-dimensional correction method, along with the finite volume method, is employed for solving the inverse problem. A series of two-dimensional and three-dimensional numerical experiments are conducted to verify the effectiveness of the method. The effects of the factors such as the temperature measurement error, the stopping criterion of the iteration, and the thermal conductivity of the flat plate on the identification results of the heat flux distributions are also studied. The numerical experiments conclude that the method is simple, stable, and accurate for this inverse heat conduction problem. The identification results are not sensitive to the temperature measurement error, whether uniform or random. Better identification results can be obtained for the test pieces with small thermal conductivity, because the temperature distribution at the inspection surface of this small conductivity plate has a larger temperature difference, which more easily reflects the distribution rule of the heat flux.

Nomenclature

e	=	uniform measurement error
h	=	film coefficient
k	=	thermal conductivity
L	=	dimension of the flat plate
m	=	discrete point number
n	=	iteration number
Q	=	matrix of heat flux distribution
Q'	=	matrix of the first-order correction term
Q''	=	matrix of the second-order correction term
q	=	heat flux
T	=	matrix of measured temperature distribution
T	=	temperature
ε	=	stopping criterion of the iteration
σ	=	standard deviation of temperature measurement

Subscripts

o	=	original measured temperature
1D	=	one-dimensional

I. Introduction

THERE are many industrial processes in which one has to adjust the thermal state of the system by manipulating heat flux through the system boundary. Some examples are the heat treatment of ingots in the soaking pit of a steel mill [1] and the baking of ceramic wafers for annealing, oxidation, and chemical vapor deposition [2]. In these cases, the amount of heat flux imposed on the boundary determines the temperature distribution in the system, and therefore the accurate determination of heat flux is a crucial step in the operation of the process. This kind of heat flux determination based on the temperature measurements at the interior points or the outer surfaces of a system belongs to the inverse heat conduction problem (IHCP).

Received 7 May 2008; revision received 3 February 2009; accepted for publication 3 February 2009.

*Lecturer, Department of Power Engineering; c.fan@hotmail.com.
†Professor, Department of Power Engineering.

Many methods have been developed for the inverse heat flux determination problem. Based on the Kalman filtering and the Karhunen–Loève Galerkin procedure, Park and Jung [3] developed an efficient real-time scheme to estimate the unsteady, spatially varying wall heat flux in a two-dimensional heat conduction system from the temperature measurement inside the domain, and numerical examples certified the effectiveness of this method. The conjugate gradient method was also used by Huang and Chen [4], Huang and Wang [5], Loulou and Scott [6], Groβ et al. [7], and Yang et al. [8] for the determination of the heat flux distribution or its variation with time. In their work, the conjugate gradient method was used to update the heat flux estimation until the convergence of the estimated and the measured temperature distributions. Bialecki et al. [9] solved the reconstruction problem of the time-dependent boundary heat flux based on the Levenberg–Marquardt method along with the boundary element method. Confident results were obtained for the numerical examples of the problem over an airfoil. The Levenberg–Marquardt method was also used by Su et al. [10] for the estimation of the spatially nonuniform wall heat flux in turbulent circular-pipe flow.

In this paper, a simple and stable numerical method is presented for estimating the heat flux distribution in a multidimensional inverse heat conduction problem. The method employed is the modified one-dimensional correction method (MODCM) [11,12], which is a simple but accurate inverse method that can deal with the multidimensional inverse heat conduction problem by using a one-dimensional inverse function. The discrepancy of the estimated results caused by the one-dimensional simplification is then corrected during the iteration process. Our previous study [11,12] demonstrated that this method can yield good estimates of the interfacial geometry of a multiple-region domain and the effective thermal conductivity distribution of the interlayer of a sandwich plate based on thermographic temperature measurement. Hence, it is expected that the method can offer a new alternative for the heat flux distribution identification problems, especially for three-dimensional problems. A series of numerical experiments are conducted in the paper to verify the effectiveness of the method. Meanwhile, the effects of the factors such as the temperature measurement error, the stopping criterion of the iteration, and the thermal conductivity of the flat plate on the identification results of the heat flux distributions are also studied.

II. Mathematical Formulation of the Problem

The problem to be considered is illustrated in Fig. 1. A nonuniform heat flux is applied to the plate from the left surface. From the

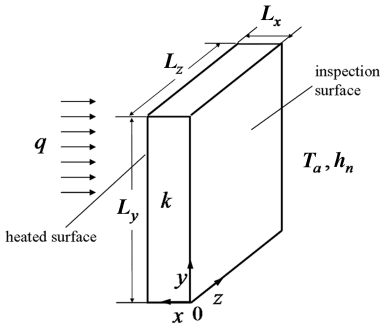

Fig. 1 Three-dimensional inverse heat conduction problem to be solved for the heating flux distribution $q(y, z)$.

inspection surface (i.e., the right surface), heat is dissipated into ambient by natural convection. For simplification, a constant film coefficient h_n is adopted for this inspection surface in this paper. The other four surfaces are insulated. The ambient temperature is T_a. The size of the flat plate is described by L_x, L_y, and L_z in the x, y, and z directions, respectively. The temperature distribution at the inspection surface is measured by an infrared imager or thermocouples. The temperature measurement along with the known geometrical and thermophysical data give rise to the inverse heat conduction problem, which can be mathematically described by the following steady-state governing equation and boundary conditions for the flat plate:

$$\frac{\partial^2 T}{\partial x^2} + \frac{\partial^2 T}{\partial y^2} + \frac{\partial^2 T}{\partial z^2} = 0 \tag{1}$$

Boundary conditions:

$$\begin{cases} k\frac{\partial T}{\partial x}|_{x=0} = h_n(T - T_a); \quad k\frac{\partial T}{\partial x}|_{x=L_x} = q(y, z) \\ \frac{\partial T}{\partial y}|_{y=0} = \frac{\partial T}{\partial y}|_{y=L_y} = 0 \\ \frac{\partial T}{\partial z}|_{z=0} = \frac{\partial T}{\partial z}|_{z=L_z} = 0 \end{cases} \tag{2}$$

where k is the thermal conductivity of the plate.

In the inverse problem, all parameters illustrated in Fig. 1 are known except the heating flux distribution $q(y, z)$. The goal of the IHCP solution is to determine the heat flux distribution $q(y, z)$ based on the temperature measurement of the inspection surface.

III. MODCM

A. Introduction of the MODCM

The MODCM is developed in our previous work based on the one-dimensional correction method (ODCM) presented by Yang et al. [13] by correcting the iteration function, modifying the calculation of the correction terms, and giving the stopping criterion of the iteration [11,12]. The MODCM first calculates the parameters to be determined for the multidimensional inverse problem based on a one-dimensional inverse function. Then the discrepancy caused by the one-dimensional simplification is corrected by iteration. The expression of the iteration function is developed based on the Taylor's series expansion.

For the inverse problem considered in this paper, the heat flux distribution $q(y, z)$ is described by a matrix Q formed by the discrete flux value:

$$q_{i,j}\ (i = 1 \sim m_y;\ j = 1 \sim m_z)$$

where m_y and m_z are the numbers of the node layers in the y and z directions, respectively, and $q_{i,j}$ is first calculated based on the corresponding discrete measured temperature value

$$T_{oi,j}(i = 1 \sim m_y;\ j = 1 \sim m_z)$$

of the inspection surface (i.e., the element of the measured temperature matrix T_o), according to the one-dimensional inverse function $q_{1D}(T)$, which can be deduced easily from the one-dimensional heat conduction problem.

The Taylor's series expansion at an arbitrary temperature $\hat{T}$ has the following form:

$$p(T) = p(\hat{T}) + p'(\hat{T})(T - \hat{T}) + \frac{p''(\hat{T})}{2!}(T - \hat{T})^2 + \cdots + \frac{p^{(n+1)}(\xi)}{(n+1)!}(T - \hat{T})^{n+1} \tag{3}$$

Therefore, for the problem of concern in this paper, the heat flux distribution of the left surface can be updated on the basis of the initial estimation $q_{i,j}(T_{i,j})$ for each discrete point by

$$q_{i,j}(T_{oi,j}) \approx q_{i,j}(T_{i,j}) + q'_{i,j}(T_{i,j})(T_{oi,j} - T_{i,j}) + \frac{q''_{i,j}(T_{i,j})}{2!}(T_{oi,j} - T_{i,j})^2 = q_{i,j}(T_{oi,j})|_{\text{initial}} + q'_{i,j}(T_{i,j})(T_{oi,j} - T_{i,j}) + \frac{q''_{i,j}(T_{i,j})}{2!}(T_{oi,j} - T_{i,j})^2 \tag{4}$$

where $T_{i,j}$ is the temperature distribution at the inspection surface calculated according to the multidimensional Eq. (1) based on the initial estimation of the heat flux distribution, and the subscript o denotes the original temperature measurement. Of course, the precise estimation cannot be obtained by using Eq. (4) once. Then from Eq. (4), a iterative corrective function can be derived for updating $q_{i,j}(T_{oi,j})$ as

$$q^{n+1}_{i,j}(T_{oi,j}) \approx q^n_{i,j}(T_{oi,j}) + q'^n_{i,j}(T^n_{i,j})(T_{oi,j} - T^n_{i,j}) + \frac{q''^n_{i,j}(T^n_{i,j})}{2!}(T_{oi,j} - T^n_{i,j})^2 \tag{5}$$

where $q'^n_{i,j}$ and $q''^n_{i,j}$ are determined for each iteration through numerical calculations, the superscript n is the iteration number, and $T^n_{i,j}$ is the calculated temperature distribution at the inspection surface according to the multidimensional Eq. (1) based on the estimated heat flux $q^n_{i,j}(T_{oi,j})$ of the last iteration.

When the matrixes formed by the elements $q'_{i,j}$ and $q''_{i,j}$ are also expressed as matrixes Q and Q'' for each iteration, the iteration process in Eq. (5) can then be rewritten as

$$\mathsf{Q}^{n+1} = \mathsf{Q}^n + \mathsf{Q}'^n * (\mathsf{T}_o - \mathsf{T}^n) + \frac{\mathsf{Q}''^n}{2!} * (\mathsf{T}_o - \mathsf{T}^n) * (\mathsf{T}_o - \mathsf{T}^n) \tag{6}$$

If the last term is neglected, Eq. (6) becomes

$$\mathsf{Q}^{n+1} = \mathsf{Q}^n + \mathsf{Q}'^n * (\mathsf{T}_o - \mathsf{T}^n) \tag{7}$$

where Q^n is the nth estimated result of the heat flux distribution after $n-1$ iterations, T^n is a matrix describing the temperature

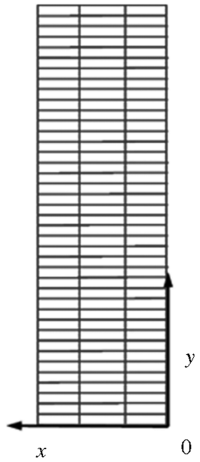

Fig. 2 Schematic of grid meshing of the plate for two-dimensional test cases.

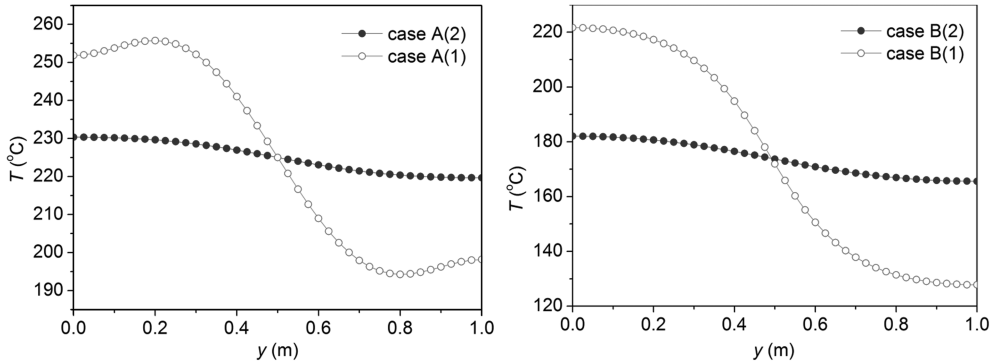

Fig. 3 Temperature distributions at the inspection surface for test case A and case B.

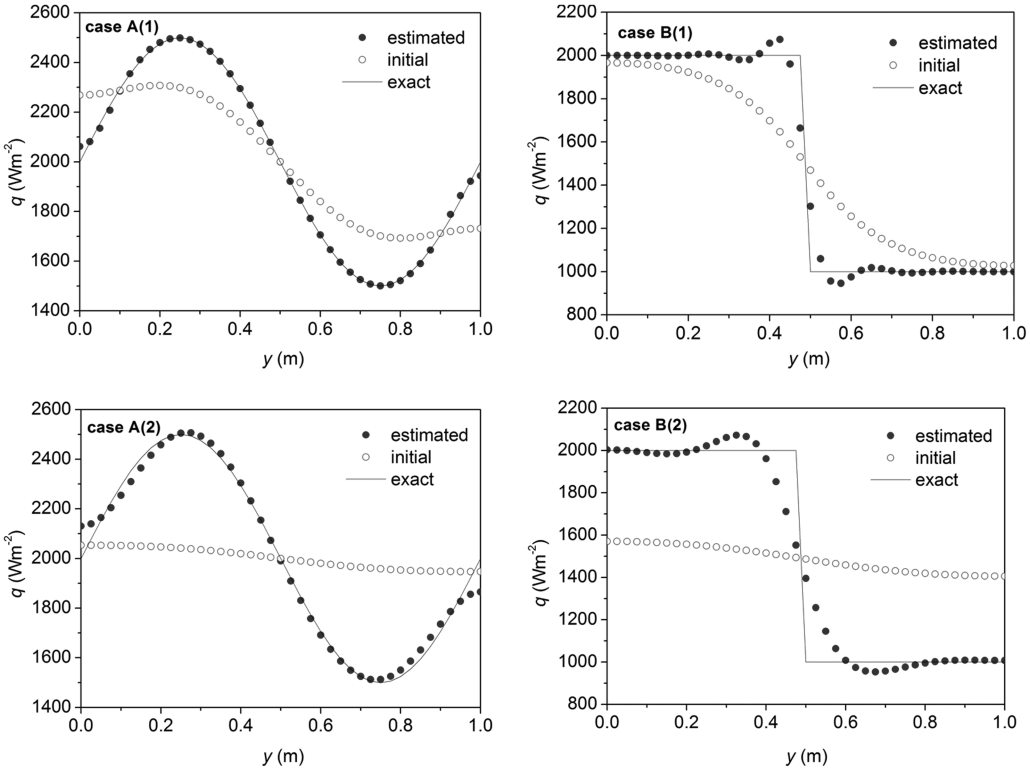

Fig. 4 Identification results of the heat flux distribution when no measurement error is considered for case A and case B ($\varepsilon = 0.1$).

distribution at the inspection surface when the heat flux distribution of the left surface is Q^n, T_o is the original measured temperature distribution at the inspection surface, Q' and Q'' are the correction terms, the symbol $*$ in Eqs. (6) and (7) denotes the Hadamard product (i.e., the element by element product) of two matrixes with the same size, and the superscript n is the iteration number. In Eqs. (6) and (7), the matrixes Q, Q', Q'', T_o, and T have the same size $m_y \times m_z$.

B. Obtainment of Correction Terms

The two terms Q' and Q'' in Eq. (6) or Eq. (7) should be determined in each iteration to refine the identification result of the heat flux distribution. Based on [13], the elements of these two matrixes can be determined approximately based on the following equations:

$$\begin{cases} q'_{i,j}(T_{i,j}) \approx \Delta q_{i,j}/\Delta T_{i,j} \\ q''_{i,j}(T_{i,j}) \approx \Delta q'_{i,j}/\Delta T_{i,j} \end{cases} \tag{8}$$

For the MODCM, the term $q'_{i,j}(T_{i,j})$ of each iteration is computed as follows:

1) Perturb the element $q_{i,j}$ of the heat flux distribution matrix Q obtained from the last iteration one by one.

2) Compute the resulting change in the temperature $T_{i,j}$ of the corresponding point on the inspection surface from the solution of the multidimensional heat conduction problem described by Eq. (1).

3) Calculate the ratio of the two perturbations $\Delta q_{i,j}$ and $\Delta T_{i,j}$ according to Eq. (8).

From Eq. (8), one can see that the computational process for the term $q''_{i,j}(T_{i,j})$ is relatively complicated. Fortunately, our previous numerical experiments showed that there is not much difference in the result of the inverse heat conduction problem whether Eq. (6) or Eq. (7) is used. Using Eq. (6) can only slightly decrease the iteration number, but will also increase the computational time of each iteration; therefore, in most cases, Eq. (7) is commonly used to solve the inverse heat conduction problem.

C. Stopping Criterion of the Iteration

The stopping criterion of the iteration of the MODCM is

$$J(\mathsf{Q}) = \sum_{i=1}^{m_y}\sum_{j=1}^{m_z}[T_{oi,j} - T^n_{i,j}]^2 < \varepsilon \tag{9a}$$

where ε is a small positive number; m_y and m_z denote the number of the node layers in the y and z directions, respectively; and the

Table 1 Relationship between the ARE of the identification result and the stopping criterion

	ARE, %			
ε	Case A(1)	Case B(1)	Case A(2)	Case B(2)
1	0.5	2.5	1.7	5.6
0.1	0.3	2.1	1.3	4.5
0.01	0.2	1.6	0.8	3.9
0.001	0.2	1.3	0.6	3.2

superscript n is the iteration number. When the random error of the temperature measurement is considered, the discrepancy principle [14,15] is used and the stopping criterion becomes

$$J(\mathbf{Q}) = \sum_{i=1}^{m_y}\sum_{j=1}^{m_z}[T_{oi,j} - T_{i,j}^n]^2 < \varepsilon = m_y m_z \sigma^2 \tag{9b}$$

where σ is the standard deviation of the temperature measurements.

D. Computational Procedure of the MODCM

Calculate the initial heat flux distribution $\mathbf{Q}^1$ based on the measured temperature distribution $\mathbf{T}_o$ at the inspection surface by using the one-dimensional inverse function $q_{1D}(T)$ to begin the iteration process. Suppose that $\mathbf{Q}^n$ is obtained after $n-1$ iterations.

1) Compute the temperature distribution $\mathbf{T}^n$ at the inspection surface based on the estimated heat flux distribution $\mathbf{Q}^n$ of the left surface according to the multidimensional heat transfer problem in Eq. (1).

2) Check the stopping criterion given by Eq. (9), and print the result if satisfied.

3) Compute the correction terms $\mathbf{Q}'^n$ and $\mathbf{Q}''^n$ in accordance with Eq. (8) based on the heat flux distribution $\mathbf{Q}^n$ by the perturbation method described in Sec. III.B.

4) Calculate the new heat flux distribution $\mathbf{Q}^{n+1}$ based on Eq. (7), and return to step 1.

IV. Numerical Experiments and Discussion

To verify the validity of the MODCM in identifying the heat flux distribution, a series of two-dimensional and three-dimensional numerical examples with different heat flux distributions are considered in this section. In all test cases, the parameters are selected as $T_a = 25°\text{C}$, $L_x = 0.2$ m, $L_y = 1.0$ m, $L_z = 1.0$ m, and $h_n = 10\ \text{Wm}^{-2}\cdot\text{K}^{-1}$. Equation (1) is solved by the finite volume method [16]. The number of node layers of the flat plate in the x direction is 4. For the two-dimensional study, the number of the node layers in the y direction m_y is set as 41, which is shown schematically in Fig. 2. For the three-dimensional study, the numbers in both the y and z directions are 21: namely, $m_y = 21$ and $m_z = 21$. In the numerical experiments, the measured temperature distribution $\mathbf{T}_o$ at the inspection surface is simulated by the solution of the multidimensional Eq. (1), based on the known heat flux distribution of the left surface to be determined and to which errors can be added to simulate the real temperature measurement. Based on these simulated measurement data, the identification work is conducted, and the result will be compared with the known exact heat flux distribution to verify the effectiveness of the algorithm.

To describe the precision level of the identification results, an average relative error (ARE) is also defined by comparing the estimated and the exact (known) heat flux distributions of the left surface as

$$\text{ARE} = \frac{1}{m_y m_z}\sum_{i=1}^{m_y}\sum_{j=1}^{m_z}\left|\frac{q_{i,j} - \hat{q}_{i,j}}{\hat{q}_{i,j}}\right| \times 100\% \tag{10}$$

where $q_{i,j}$ is the estimated result, and $\hat{q}_{i,j}$ denotes the known distribution of the heat flux applied to the left surface of the plate.

The one-dimensional inverse function $q_{1D}(T)$, which will be used to calculate the initial heat flux distribution, can be derived based on the measured temperature T of the inspection surface according to the energy conservation in the one-dimensional heat transfer problem as

$$q_{1D}(T) = q(T) = h_n(T - T_a) \tag{11}$$

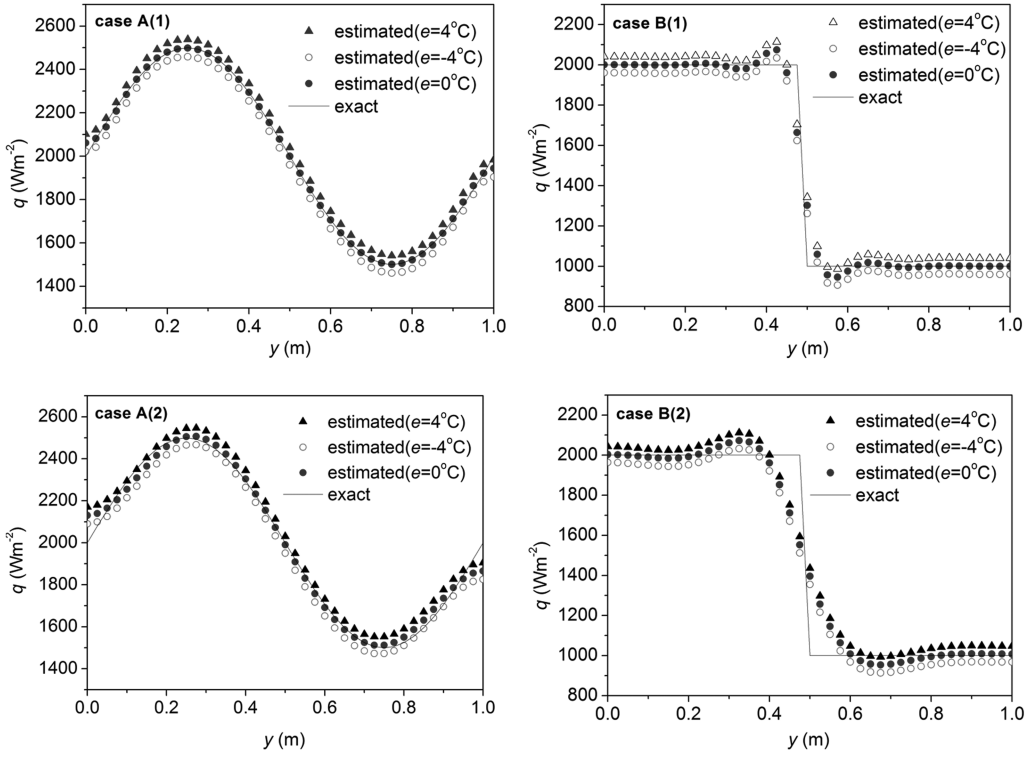

Fig. 5 Identification results of the heat flux distribution with measurement error in consideration for case A and case B ($\varepsilon = 0.1$).

Table 2 Relationship between the measurement error and the ARE of identification results

	ARE, %			
e, °C	Case A(1)	Case B(1)	Case A(2)	Case B(2)
−2	1.2	3.0	1.6	5.0
2	1.2	3.0	1.7	5.0
−4	2.2	4.3	2.3	5.9
4	2.2	4.3	2.5	5.9

A. Two-Dimensional Numerical Test Cases

If the dimension of the flat plate in the z direction is very long relative to those in the y and x directions and the heat flux added to the left surface of the plate does not change in the z direction either, the IHCP of determining the heat flux distribution can be deemed to be two-dimensional.

For this two-dimensional problem, the functions of the heat flux changing in y direction of the two test cases are as follows:

Case A:

$$q(y) = 2000 + 500\sin(2\pi y/L_y); \qquad 0 \le y \le L_y \tag{12}$$

Case B:

$$q(y) = \begin{cases} 2000; & 0 \le y \le 21L_y/41 \\ 1000; & 21L_y/41 < y \le L_y \end{cases} \tag{13}$$

To study the effect of the thermal conductivity of the test piece on the estimation of the heat flux distribution, two thermal conductivities are adopted: one is 0.1 $\mathrm{Wm^{-1}\cdot K^{-1}}$ and the other is 30 $\mathrm{Wm^{-1}\cdot K^{-1}}$. The numerical examples corresponding to these two conductivities are denoted by cases A(1) and B(1) and cases A(2) and B(2), respectively. Based on Eq. (1), the temperature distributions at the inspection surface are calculated numerically by the finite volume method and plotted in Fig. 3. Based on these temperature distribution curves (i.e., the simulated measurement data), the identification work is conducted to certify the effectiveness of the inverse method.

When no measurement error is considered, the identification results of the heat flux distribution of the left surface of the plate are shown in Fig. 4. The exact curves in the figures are the known heat flux distributions described in Eqs. (12) and (13). The stopping criterion is set as $\varepsilon = 0.1$. The estimated and the exact curves have a good agreement. Though the AREs for the test cases B(1) and B(2) are relative larger, the largest value is still less than 5%. In the figures, the initial identification results of the heat flux are also shown, which were obtained only by using the one-dimensional inverse function (11) before the iteration begins. These initial curves tell us that one-dimensional simplification will cause obvious discrepancy in the identification results; therefore, the iterative correcting process is necessary.

The relationship between the ARE of the identification result and the stopping criterion of the iteration process is studied systematically in Table 1. The ARE increases with the increase of the stopping criterion. When $\varepsilon \le 0.1$, the AREs of the identification results are smaller than 5%; therefore, $\varepsilon = 0.1$ is good enough to be used in the following numerical examples in this subsection. From the table, we also can see that the result for the test piece with smaller conductivity is more accurate, because the temperature distribution at the inspection surface of this small conductivity plate, as is shown in Fig. 3, has a larger temperature difference, which more easily reflects the distribution rule of the heat flux applied to the left surface.

In this section, the effect of the uniform temperature measurement error that corresponds to the thermographic temperature measurement is studied. In Fig. 5, the estimated heat flux distributions are plotted for the four numerical examples when the uniform measurement errors e are +4 and −4°C, respectively. More details of the AREs of the identification results when the measurement error is considered are reported in Table 2. Here, $e = 2$ and 4°C represent about 1.0 and 2.0% of the average measured temperature, respectively. From the figures and the table, one can see that the AREs of identification results increase with the increase of the measurement error. The identified heat flux distribution curve moves up or down along the vertical axis, which depends on the sign of the measurement error. When the absolute value of measurement error is less than 4°C, the effect of the measurement error on the identification result can be neglected, because the AREs of the identification results are smaller than 6.0%.

As stated in our previous work [12], for the MODCM, when the uniform measurement error is added to the temperature distribution at the inspection surface, a new test case is formed with this new simulated temperature measurement, but the precision level of the method remains unchanged as long as the stopping criterion is the same. A numerical example for solving this heat flux identification problem is also presented in this section to prove this. In Fig. 6, the temperature distributions at the inspection surface are plotted, which were obtained according to Eq. (1) based on the exact heat flux distribution and that estimated when the measurement errors of the

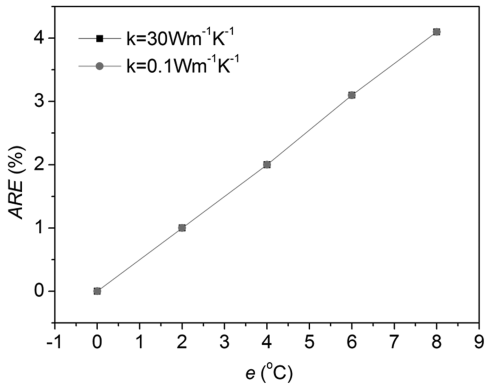

Fig. 7 The ARE of the heat flux calculated analytically based on the inverse Eq. (11) when the heat flux applied is uniform in the y–z plane of Fig. 1.

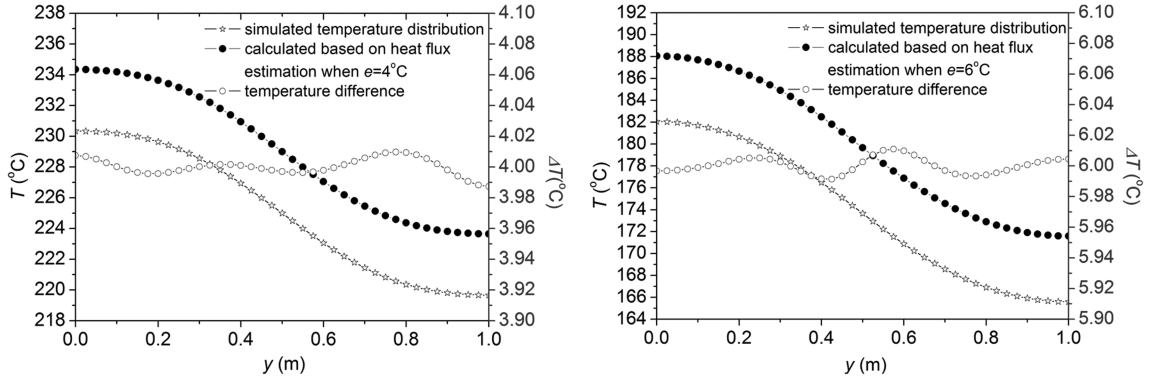

Fig. 6 Temperature distributions calculated based on the exact and the estimated heat flux distributions and their differences.

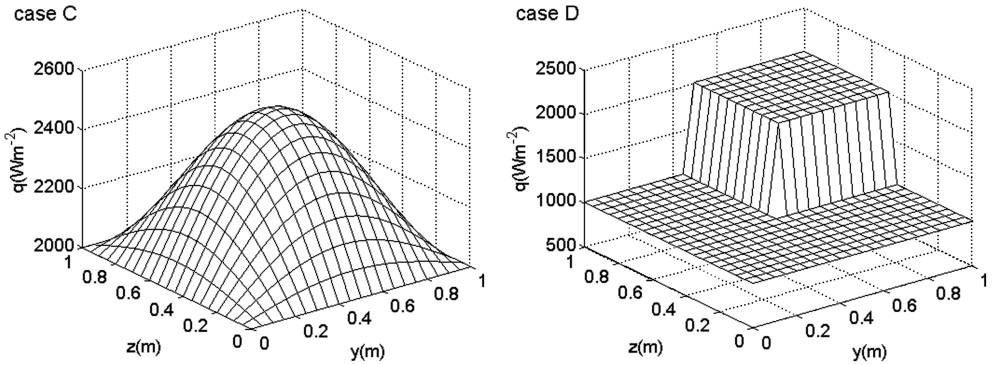

Fig. 8 Exact heat flux distributions to be determined for case C and case D.

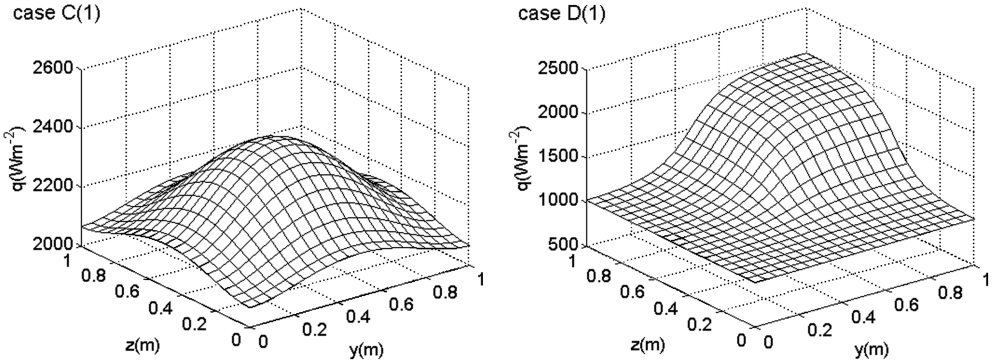

Fig. 9 Initial identification results of heat flux distributions for cases C(1) and D(1) according to function (11).

temperature are +4 and even +6.0°C. From the figures, one can see that both differences between two temperature curves for case A(2) and case B(2) are 4 ± 0.02 and 6 ± 0.02°C, respectively.

When the heat flux distribution of the left surface does not change in the y–z plane of Fig. 1, the identification problem becomes one-dimensional and its analytical solution can be obtained from Eq. (11). The AREs of this analytical solution in Fig. 7 for the heat flux distribution $q(y, z) = 2000$ Wm^{-2} when the temperature measurement error of the inspection surface ranges from 0 to 8°C also proved that the error described in Table 2 is mostly the nature of this inverse problem, not a result of the numerical method.

Note that this error is a definite value and can be eliminated only if the temperature measurement error can be estimated precisely. For the analysis and estimation of the thermographic temperature measurement error, one can refer to our previous work [17–19].

B. Three-Dimensional Numerical Test Cases

In this section, the numerical method is tested for solving the three-dimensional IHCP for determining the distribution of the heat flux applied to the left surface of the plate shown in Fig. 1. The heat flux distributions to be determined are shown in Fig. 8. Two conductivities, 1.0 and 10.0 Wm$^{-1} \cdot$ K^{-1}, of the plate are adopted for both cases C and D. As in the two-dimensional cases, the test cases are numbered as C(1) and D(1) with the former conductivity and C(2) and D(2) with the latter. Based on the simulated temperature distribution at the inspection surface, which is obtained according to Eq. (1), the heat flux distribution is first estimated based on the inverse function (11), and the results of cases C(1) and D(1) are plotted in Fig. 9 as examples. Then the discrepancy caused by using this one-dimensional inverse function is corrected by the iteration process according to Eq. (7). The AREs of the identification results for the four test cases when the stopping criterion is adopted as $\varepsilon = 0.1$ are listed in Table 3. The results of the two test cases C(1) and D(1) are also plotted in Fig. 10. From the figures and table, it is easy to see that the estimated and the exact heat flux distributions have a very good agreement when no temperature measurement error is considered.

When the random error of the temperature measurement (which corresponds to individual measurement for every discrete point on the inspection surface, such as those using thermocouples) is added to the exact temperature distribution, a temperature curve with sharp changes within the range of $-\sigma \sim \sigma$ is obtained. Because the heat transfer in the plate has a smooth character, the temperature distribution with sharp changes of the inspection surface is impossible to obtain, regardless of the heat flux distribution; therefore, it is meaningless to expect the stopping criterion $J(\mathbf{Q})$ in Eq. (9a) to be zero. In this paper, the stopping criterion based on the discrepancy principle, which is related to the standard deviation of temperature measurement and also to the discrete point number, is used to measure the acceptable convergence between the calculated and the measured temperature distributions.

In Figs. 11 and 12, the identification results of the heat flux distributions in cases C(1) and D(1) are plotted when random errors of the temperature measurement at the inspection surface are considered, and more details on the AREs of the identification results for different measurement errors and different plate conductivities are reported in Table 3. The stopping criterion of the iteration is calculated based on Eq. (9b). From both the figures and the table, one can see that confident identification results can still be obtained when random error is considered and that the identification results are not sensitive to the temperature measurement error of the inspection surface, because the largest ARE is not more than 12.1% [20].

Table 3 Relationship between the ARE and the standard deviation of the measurement

	ARE, %			
σ, °C	Case C(1)	Case D(1)	Case C(2)	Case D(2)
0.0	0.2	0.6	0.5	1.0
0.5	0.9	4.5	2.0	7.4
1.0	1.3	5.6	2.8	9.1
2.0	1.8	6.7	3.9	10.8
3.0	2.4	8.1	5.0	12.1

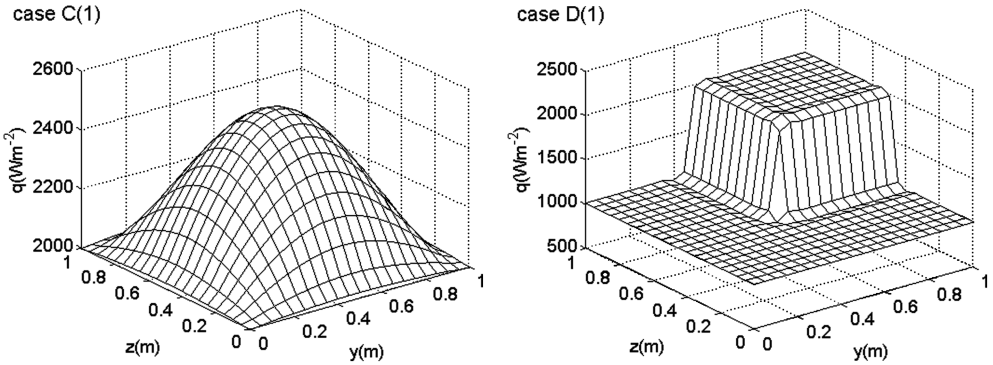

Fig. 10 Final identification results of heat flux distributions for cases C(1) and D(1) ($\varepsilon = 0.1$).

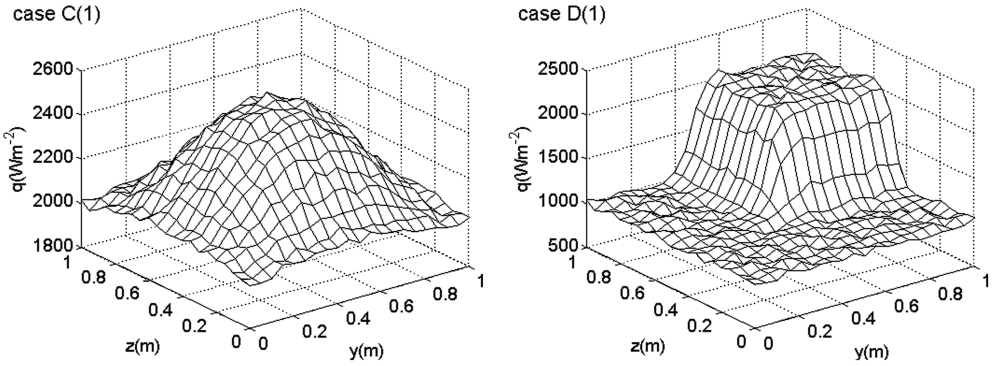

Fig. 11 Identification results of heat flux distributions for cases C(1) and D(1) with random measurement error in consideration ($\sigma = 0.5$°C).

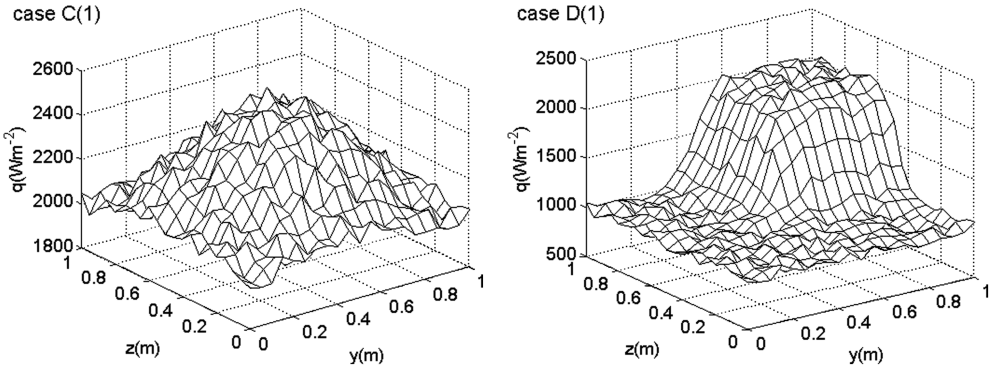

Fig. 12 Identification results of heat flux distributions for cases C(1) and D(1) with random measurement error in consideration ($\sigma = 2.0$°C).

From the preceding two- and three-dimensional test cases, it was concluded that the MODCM is now applied successfully in this multidimensional inverse heat conduction problem for predicting the unknown steady heat flux distribution. The identification results are not sensitive to the temperature measurement error of the inspection surface. More accurate identification results can be obtained when the flux distribution has no sharp changes and also when the thermal conductivity of the test piece is smaller.

V. Conclusions

The modified one-dimensional correction method was successfully applied for the solution of the inverse heat conduction problem to determine the unknown heat flux distribution by using the temperature readings at the inspection surface of a flat plate. Several test cases involving different functional forms of the unknown heat flux distribution and different measurement errors were considered. The numerical testing results conclude that the identification results with high accuracy can be obtained when no measurement error at the inspection surface is considered and that the identification results are not sensitive to the measurement error, whether uniform or random. Our future work is the identification of unsteady boundary conditions.

Acknowledgment

The authors would like to acknowledge the financial support from the Natural Science Foundation of the Naval University of Engineering, grant number HGDJJ05009.

References

[1] Lausterer, G. K., and Ray, W. H., "Distributed Parameter State Estimation and Optimal Feedback Control—An Experimental Study in Two Space Dimensions," *IEEE Transactions on Automatic Control*, Vol. 24, 1979, pp. 179–189. doi:10.1109/TAC.1979.1101997

[2] Nulman, J., Krusius, J. P., and Gat, A., "Rapid Thermal Processing of Thin Gate Dielectrics-Oxidation of Silicon," *IEEE Electron Device Letters*, Vol. 6, 1985, pp. 205–208. doi:10.1109/EDL.1985.26099

[3] Park, H. M., and Jung, W. S., "Multidimensional Inverse Heat Conduction Problems Using an Efficient Sequential Method," *Journal*

of Heat Transfer, Vol. 123, No. 6, 2001, pp. 1021–1029.
doi:10.1115/1.1409260

[4] Huang, C. H., and Chen, W. C., "A Three Dimensional Inverse Forced Convection Problem in Estimating Surface Heat Flux by Conjugate Gradient Method," *International Journal of Heat and Mass Transfer*, Vol. 43, No. 17, 2000, pp. 3171–3181.
doi:10.1016/S0017-9310(99)00330-0

[5] Huang, C. H., and Wang, S. P., "A Three-Dimensional Inverse Heat Conduction Problem in Estimating Surface Heat Flux by Conjugate Gradient Method," *International Journal of Heat and Mass Transfer*, Vol. 42, No. 18, 1999, pp. 3387–3403.
doi:10.1016/S0017-9310(99)00020-4

[6] Loulou, T., and Scott, E. P., "Estimation of 3-Dimensional Heat Flux from Surface Temperature Measurements Using an Iterative Regularization Method," *Heat and Mass Transfer*, Vol. 39, Nos. 5–6, 2003, pp. 435–443.

[7] Groβ, S., Soemers, M., Mhamdi, A., Sibai, F. A., Reusken, A., Marquardt, W., and Renz, U., "Identification of Boundary Heat Fluxes in a Falling Film Experiment Using High Resolution Temperature Measurements," *International Journal of Heat and Mass Transfer*, Vol. 48, No. 25-26, 2005, pp. 5549–5562.
doi:10.1016/j.ijheatmasstransfer.2005.06.030

[8] Yang, Y. C., Wu, T. S., and Wei, E. J., "Modeling of Simultaneous Estimating the Laser Heat Flux and Melted Depth During Laser Processing by Inverse Methodology," *International Communications in Heat and Mass Transfer*, Vol. 34, No. 4, 2007, pp. 440–447.
doi:10.1016/j.icheatmasstransfer.2007.01.010

[9] Bialecki, R., Divo, E., and Kassab, A., "Reconstruction of Time-Dependent Boundary Heat Flux By a BEM-Based Inverse Algorithm," *Engineering Analysis with Boundary Elements*, Vol. 30, No. 9, 2006, pp. 767–773.
doi:10.1016/j.enganabound.2006.04.001

[10] Su, J., Lopes, A. B., and Neto, A. J. S., "Estimation of Unknown Wall Heat Flux in Turbulent Circular Pipe Flow," *International Communications in Heat and Mass Transfer*, Vol. 27, No. 7, 2000, pp. 945–954.
doi:10.1016/S0735-1933(00)00174-3

[11] Fan, C., Sun, F., and Yang, L., "An Algorithm Study on Inverse Identification of Interfacial Configuration in a Multiple Region Domain," *Journal of Heat Transfer*, Vol. 131, No. 2, 2009, Paper 021301.
doi:10.1115/1.2994765

[12] Fan, C., Sun, F., and Yang, L., "A Numerical Method for Determining Thermal Conductivity Distribution of the Interlayer of a Sandwich Plate Based on Thermographic Temperature Measurement," *Journal of Physics D: Applied Physics*, Vol. 41, 2008, Paper 135501.
doi:10.1088/0022-3727/41/13/135501

[13] Yang, L., Geng, W., Jiang, L., Zou, L., and Hong, J., "Profile Reconstruction in Dynamic Infrared Thermography: Adaptability and Stability," *International Journal of Infrared and Millimeter Waves*, Vol. 20, No. 4, 1999, pp. 623–634.
doi:10.1023/A:1022644623243

[14] Ozisik, M. N., and Orlande, H. R. B., *Inverse Heat Transfer—Fundamentals and Applications*, Taylor and Francis, New York, 2000, pp. 35–114.

[15] Alifanov, O. M., *Inverse Heat Transfer Problems*, Spring–Verlag, New York, 1994.

[16] Guo, K., *Numerical Heat Transfer*, Science and Technology Press, Hefei, China, 1987.

[17] Yang, L., "Calculation and Error Analysis of Temperature Measurement Using Thermal Imager," *Infrared Technology*, Vol. 21, No. 4, 1999, pp. 20–24 (in Chinese).

[18] Kou, W., and Yang, L., "Error Analysis of Infrared Measurement," *Infrared Technology*, Vol. 23, No. 3, 2001, pp. 32–35 (in Chinese).

[19] Fan, C., Sun, F., and Yang, L., "Temperature Distribution Rules of Equipment Surface with Subsurface Defect and Effect of Natural Convective Heat Transfer in Defect to Thermographic Inspection," *Laser and Infrared*, Vol. 35, No. 7, 2005, pp. 504–507 (in Chinese).

[20] Huang, C. H., and Shih, C. C., "Identify the Interfacial Configurations in a Multiple Region Domain Problem," *Journal of Thermophysics and Heat Transfer*, Vol. 19, No. 4, 2005, pp. 533–541.
doi:10.2514/1.11260